Mutants of Ubiquinol–Cytochrome c_2 Oxidoreductase Resistant to Q_o Site Inhibitors: Consequences for Ubiquinone and Ubiquinol Affinity and Catalysis†

Dan E. Robertson,*,‡ Fevzi Daldal,§ and P. Leslie Dutton‡

Department of Biochemistry and Biophysics, School of Medicine, and Department of Biology, University of Pennsylvania, Philadelphia, Pennsylvania 19104

Received May 30, 1990; Revised Manuscript Received August 27, 1990

ABSTRACT: Seven single-site mutants in six residues of the cyt *b* polypeptide of *Rhodobacter capsulatus* selected for resistance to the Q_o site inhibitors stigmatellin, myxothiazol, or mucidin [Daldal, F., Tokito, M. K., Davidson, E., & Faham, M. (1989) *EMBO J. 8*, 3951–3961] have been characterized by using optical and EPR spectroscopy and single-turnover kinetic analysis. The strains were compared with wild-type strain MT1131 and with the Ps^- strain R126 (G158D), which is dysfunctional in its Q_o site [Robertson, D. E., Davidson, E., Prince, R. C., van den Berg, W. H., Marrs, B. L., & Dutton, P. L. (1986) *J. Biol. Chem. 261*, 584–591]. Mutants selected for stigmatellin resistance induced a weakening in the binding of the inhibitor without discernible loss of ubiquinone(Q)/ubiquinol(QH_2) binding affinity to the Q_o site or kinetic impairment to catalysis. Mutants selected for myxothiazol or mucidin resistance, inducing weakening of inhibitor binding, all displayed impaired rates of Q_o site catalysis: The most severe cases (F144L, F144S) displayed loss of affinity for Q, and evidence suggests that parallel loss of affinity for the substrate QH_2 was incurred in these strains. The results provide a view of the nature of the interaction of Q and QH_2 of the Q_{pool} with the Q_o site. Consideration of the mutational substitutions and their structural positions along with comparisons with the Q_A and Q_B sites of the photosynthetic reaction center suggests a model for the structure of the Q_o site.

The redox centers of the ubiquinol–cytochrome cyt c_2 oxidoreductase (cyt bc_1 complex)[1] of the purple, non-sulfur bacterial family *Rhodobacter* serve to complete the cyclic transfer of electrons initiated by light activation of the photosynthetic reaction center protein (RC). The RC generates the two substrates for the cyt bc_1 complex, ferricytochrome c_2 and QH_2. Cyt c_2 is a water-soluble protein diffusing between electron donors and acceptors exposed to the periplasm. Ubiquinone is a membrane-associated electron and proton carrier diffusing between sites of redox catalysis within the membrane. The cyt bc_1 complex reduces ferricyt c_2 and oxidizes QH_2, utilizing the approximately 250 mV of standard free energy difference between these components to catalyze charge separation and translocate protons across the chromatophore membrane, resulting in the formation of the electrochemical proton gradient, $\Delta\mu_{H^+}$.

The cyt bc_1 complex of *Rhodobacter capsulatus* is coded by the three-gene *fbc* (*pet*) operon (Daldal et al., 1987; Davidson & Daldal, 1987a,b). The photosynthetic bacterial cyt bc_1 is analogous in function to its counterparts in mitochondria and chloroplasts, differing materially only in the number of auxiliary subunits found in the isolated enzyme. The redox cofactors of the cyt bc_1 complex are associated with three polypeptide subunits. The iron–sulfur subunit contains a 2Fe2S cluster, the cyt *b* polypeptide contains two electrochemically and spectroscopically distinct *b*-type cytochrome hemes (cyts b_H and b_L; subscripts indicate high and low midpoints), and the cyt *c* subunit contains a cyt c_1 [for reviews and spectral and electrochemical details see Crofts and Wraight (1983), Crofts et al. (1983), Rich (1984), and Dutton (1986)].

The presence on the cyt bc_1 of two sites for ubiquinone redox catalysis (Mitchell, 1975, 1976) now appears well established. Mitchell named the two quinone binding sites Q_o and Q_i, on the basis of their proton output and input functions. Researchers working on the cyt bc_1 complexes of photosynthetic bacteria have called these sites Q_z and Q_c, respectively.

The Q-cycle mechanism (Mitchell, 1975, 1976) is most commonly accepted as the working hypothesis for cyt bc_1 protonmotive function. Figure 1 and its legend detail the sequence of electron transfers and show the approximate positions of the redox centers and ubiquinone binding sites of the RC and cyt bc_1. Recent evidence (Glaser & Crofts, 1984; Robertson et al., 1985; Robertson & Dutton, 1987, 1988; Ohnishi et al., 1989) supports the idea that charge separation in cyt bc_1 is, like that in the RC, effected by electron transfer only, with little or no proton (H^+) movement through the low-dielectric part of the membrane; this evidence also indicates that the Q_o and Q_i sites are located close to the aqueous interfaces of the membrane, on opposite sides. Q_o and Q_i have proven to be the sites where a variety of inhibitors act, most likely by disruption of the ubiquinone–site interaction. Antimycin, long known to inhibit cyt bc_1 function, has been shown to interact with high specificity at the Q_i site, and more recently, myxothiazol, stigmatellin, mucidin, and UHDBT have been shown to be similarly specific as Q_o site inhibitors. The model of Figure 1 is appealing in its simplicity of form, in its ability to explain the majority of experimental data in a

† Research support is acknowledged from Public Health Service Grants GM 27309 to P.L.D. and 38237 to F.D.

* Author to whom correspondence should be addressed.
‡ Department of Biochemistry and Biophysics, School of Medicine.
§ Department of Biology.

[1] Abbreviations: cyt, cytochrome; cyt bc_1, ubiquinol–cyt c_2 oxidoreductase; QH_2, ubiquinol; Q, ubiquinone; cyt b_L, low-potential cyt b_{566} of cyt bc_1; cyt b_H, high-potential cyt b_{560} of cyt bc_1; Q_o, ubiquinol oxidizing site; Q_i, ubiquinone reducing site; UHDBT, 5-undecyl-6-hydroxy-4,7-dioxobenzothiazole; HQNO, 2-heptyl-4-hydroxyquinoline *N*-oxide; UHNQ; 2-hydroxy-3-undecyl-1,4-naphthoquinone; E_h, ambient redox potential; E_m, electrochemical midpoint potential; E_{m7}, electrochemical midpoint potential at pH 7; Ps^+, photosynthetic growth positive; Ps^-, photosynthetic growth negative; RC, photosynthetic reaction center.

0006-2960/90/0429-11249$02.50/0

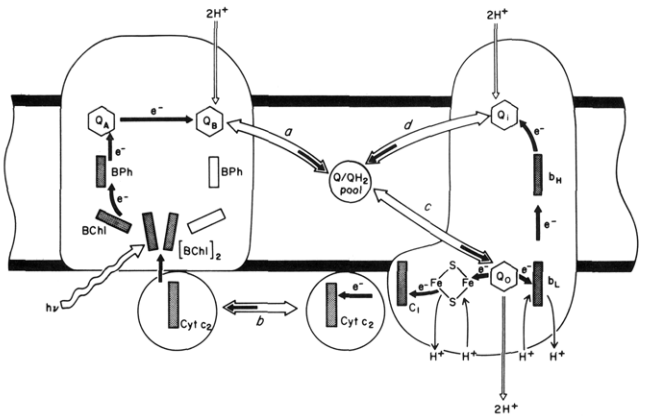

FIGURE 1: Cyclic electron-transfer system of *Rhodobacter* showing the direction of electron transfer following light absorption by $[BChl]_2$, the positions of redox centers relative to the membrane, and the relevant redox-linked protonations and deprotonations. In this model, the RC, ubiquinone in Q_{pool}, cyt bc_1, and cyt c_2, function with 2:50:1:2 stoichiometry. The sequence of the reactions in a complete turnover is as follows: (a) absorption of photons by two $[BChl]_2$ from an RC pair results in the reduction of one Q^- to QH_2 and the release of this QH_2 to Q_{pool}; (b) rereduction of two $[BChl]_2$ by two cyt c_2 provides two oxidized cyt c_2 for cyt bc_1; (c) one QH_2 from Q_{pool} is oxidized at Q_o, resulting in the reduction of one of the oxidized equivalents on cyt c_2 and 2Fe2S and reduction of (already oxidized) cyt b_L; this passes the electron onto cyt b_H which, in turn, reduces a Q from Q_{pool} at the Q_i site yielding a semiquinone at Q_i; (d) oxidation of a second QH_2 at Q_o reduces the remaining oxidizing equivalent of the cyt c_2 and 2Fe2S and results in QH_2 formation at Q_i which subsequently dissociates into Q_{pool}. The large open arrows indicate the exchanges of Q and QH_2, the large closed arrows indicate the direction of reducing equivalent flow, small open arrows refer to protonation/deprotonation of bound ubiquinone, and light, closed arrows refer to redox-linked protonation/deprotonations.

straightforward way, and as a viable model on which to frame experiments. While alternate possibilities cannot be ruled out [e.g., Konstantinov and Popova (1988)], the model of Figure 1 will remain the principal model to test and for discussing results obtained in this report.

Previous to the present study, a detailed analysis was made of *R. capsulatus* strain R126, a spontaneous nonphotosynthetic (Ps^-) mutant severely blocked in cyt bc_1 turnover (Robertson et al., 1986). The lesion was identified to be in the Q_o site, making it virtually incapable of oxidizing QH_2. Since these physical–chemical and functional analyses, the sequence alteration for R126 has been shown to be an aspartate substitution for glycine at residue 158 of the cyt *b* polypeptide, i.e., G158D (Daldal et al., 1989).

The mutants used in the current study were obtained by a different method. These were isolated as spontaneous mutants selected for resistance to the Q_o site inhibitors myxothiazol, mucidin, or stigmatellin. These three inhibitors were chosen because each causes characteristic spectral and electrochemical changes in the Q_o redox partners, 2Fe2S and cyt b_L, and because they are thought to have distinct binding determinants at the Q_o site [for a review see von Jagow and Link (1986)]. All the mutations resulting in resistance which map in *fbc* (*pet*) have been shown to map in the cyt *b* polypeptide and exhibit distinctly different patterns of cross-resistance to each of the three inhibitors (Daldal et al., 1989). These mutants are all Ps^+ so, despite the fact that large changes occur in the affinity of the cyt bc_1 for the inhibitors, drastic effects of the mutations on function, such as those encountered in mutant R126, are not anticipated. In this paper we have characterized these mutants, using the protocols developed during the R126 investigation, to explore the relationship between resistance to a particular inhibitor and what, if anything, is altered in the physical chemistry of the cofactors, the affinities of the site for ubiquinone and ubiquinol, and the kinetics of redox catalysis.

Materials and Methods

Bacterial Culture and Mutant Selection. Cultures of *R. capsulatus* were grown photosynthetically and chromatophores prepared as previously described (Dutton et al., 1975). All inhibitor-resistant strains were derived from strain MT1131, a green mutant with wild-type cyt bc_1 (Zannoni et al., 1980). Growth rates of pure cultures of mutant strains were comparable to that of strain MT1131 (Daldal et al., 1989). Mutants were selected as outlined in Daldal et al. (1989). Strain R126 was grown aerobically at low $[O_2]$ (Robertson et al., 1986). After scaling up growth of cultures on liquid medium, aliquots of each strain were routinely checked for inhibitor resistance by observing photosynthetic growth on plates prepared with the same concentrations of stigmatellin, myxothiazol, or mucidin used in the selection protocol [see Daldal et al., (1989)].

Flash-Activated Absorption Difference Spectroscopy. Flash-activated turnover of cyt bc_1 was performed on a Biomedical Instrumentation Group (University of Pennsylvania) dual-wavelength spectrophotometer fitted with an anaerobic redox cuvette. Single, short (full width at half-height, 8 μs) pulses of actinic light were delivered to the cuvette at 90° to the measuring beam. Redox potentiometry was performed as detailed in Dutton (1978). Kinetics of cyt *b* reduction were measured at 561 minus 569 nm, cyt $c_1 + c_2$ oxidation and rereduction were measured at 550 minus 540 nm, and $[BChl]_2$ oxidation–reduction was measured at 605 minus 540 nm (Dutton et al., 1975). Flash-activated kinetic transients were averaged with a Computerscope ISC-16 A/D board and software (R. C. Electronics, Inc., Santa Barbara, CA) using an IBM personal computer. Fits to kinetics traces were made with a computer program (C. C. Moser, unpublished) using the nonlinear, least-squares procedures of Bevington (1969).

The Ubiquinone Pool (Q_{pool}). The size of Q_{pool} has been determined in the closely related *Rhodobacter sphaeroides* strain Ga where it was found that approximately 35 of the 50 quinones/cyt bc_1 behaved as a homogeneous pool with an electrochemical midpoint value of 90 mV (Takamiya & Dutton, 1979). Similar measurements of pool size have been carried out in photoheterotrophically grown *R. capsulatus*, where values of 41 (Robertson et al., 1986) and 50 (Ding, Robertson, and Dutton, unpublished results) have been determined. It is clear that Q_{pool} size is a function of growth conditions, and we have therefore adopted the number 50 as the number of ubiquinones in the homogeneous pool available for interaction with cyt bc_1 and the RC. Variations in this number by 20% will have no effect on the treatment of results in the present work.

The E_{m7} for Q_{pool} in *R. capsulatus* has been determined (Ding et al., unpublished results) to be close to the midpoint determined for the closely related *R. sphaeroides* (Takamiya & Dutton, 1979), i.e., 90 mV. Thus, prior to the flash the redox state of Q_{pool} could be varied from nearly fully reduced to fully oxidized by redox poising between 30 and 200 mV. Flash activation provides an additional QH_2/cyt bc_1 to a Q_{pool} that is not fully reduced, meaning that the QH_2/cyt bc_1 ratio could be varied between 50 and 1.

Interaction of Q at the Q_o Site. The line shape of the EPR spectrum of the reduced 2Fe2S reports the redox state of Q_{pool} (Siedow et al., 1978; deVries et al., 1979; Matsuura et al., 1983a). When Q_{pool} is oxidized, the spectrum narrows, yielding

Table I

inhibitor selection	residue substitution	cyt $c_1 + c_2$ reduction: rate Q_{pool} reduced (s^{-1})	cyt $c_1 + c_2$ reduction: rate Q_{pool} oxidized (s^{-1})	cyt $c_1 + c_2$ reduction: E_h (mV) at 1/2 max rate	cyt b_H reduction rates Q_{pool} oxidized: Q_o–cyt b_H (s^{-1})	cyt b_H reduction rates Q_{pool} oxidized: Q_i–cyt b_H (s^{-1})	2Fe2S line shape, g_x	I_{50} in vitro (μM): MYX	I_{50} in vitro (μM): STG	I_{50} in vitro (μM): UHDBT
none (wt)		362 (±43)	18 (±3)	113	89 (±17)	72	1.80	0.015	<0.01	0.82
myxothiazol	G152S	301 (±23)	8 (±2)	98	68 (±8)	77	1.80	0.55	<0.02	0.90
myxothiazol	F144L	28 (±18)	4 (±2)	57	5 (±5)	84	1.765	8.00	0.05	9.00
myxothiazol	F144S	247 (±21)	13 (±3)	103	50 (±6)	79	1.80/1.78	8.00	<0.01	0.70
mucidin	L106P	72 (±19)	7 (±3)	80	49 (±11)	50	1.80	0.13	0.038	0.50
stigmatellin	V333A	387 (±52)	17 (±3)	115	72 (±13)	66	1.80	0.073	0.07	2.00
stigmatellin	T163A	403 (±28)	16 (±4)	124	78 (±11)	89	1.80	0.05	0.06	2.70
stigmatellin	M140I	378 (±61)	16 (±3)	110	85 (±12)	90	1.80	0.30	0.075	2.20
R126	G158D (Ps^- mutant)	0	0		0	ND	1.77	ND	ND	ND

a clearly observed, sharpened g_x feature centered at $g = 1.80$. When the Q_{pool} is reduced, the line shape becomes broadened and the g_x feature is centered at $g = 1.78$. Thus the 2Fe2S spectrum provides a direct measure of the occupancy of the Q_o site by Q. The EPR line shape of the 2Fe2S center was measured as outlined in Robertson et al. (1986). Samples were poised with Q_{pool} oxidized and 2Fe2S reduced by addition of 0.1 μM *N*-methyldibenzopyrazine methosulfate (PMS) and 20 mM sodium ascorbate. Q_{pool} and 2Fe2S were poised in the reduced forms by addition of sodium dithionite. Measurements were performed at 15 K at a microwave power of 1 mW on a Varian E-109 X-band spectrometer equipped for low-temperature operation with a variable-temperature, flowing helium cryostat (Air Products LTD 3-110).

Oxidation of QH_2 at the Q_o Site. QH_2 oxidation at the Q_o site was observed as outlined in eq 1, which describes the

$$Q_oH_2 + \text{ferricyt } b_H + \text{ferricyt } c_1 + c_2 \rightarrow Q_o + \text{ferrocyt } b_H + \text{ferrocyt } c_1 + c_2 + 2H^+ \quad (1)$$

generally accepted reaction catalyzed by this site after QH_2 is bound. For simplicity, the equation is restricted to the experimentally observed components, predominantly cyt b_H and cyts $c_1 + c_2$ (Figure 1). The left-hand side of the equation shows ferricyt $c_1 + c_2$ which is generated in less than 1 ms by the flash-activated RC (Meinhardt & Crofts, 1982; Moser & Dutton, 1988). Cyt b_H is poised in the oxidized form prior to activation by redox potentiometry. QH_2 is derived either from the flash-activated reaction center Q_B site if the Q_{pool} is fully oxidized or from the reduced members of Q_{pool}. Thus, the rate of arrival, binding, and oxidation of the QH_2 at the Q_o site is determined by the state of reduction of the Q_{pool}, the affinities of Q and QH_2 for Q_o, and the collisional characteristics of the ubiquinone and the site.

Complications to the measurement of the rate of QH_2 oxidation at the Q_o site arise, as is described in Figure 1, because a complete turnover of the cyt bc_1 involves the successive oxidation of two QH_2 [see Figure 1, Matsuura et al. (1983b), and Crofts et al. (1983)]. The most direct measure of the rate of a single QH_2 oxidation at the Q_o site is provided by observing the rate of cyt b_H reduction in a cyt bc_1 whose complete turnover has been inhibited by addition of antimycin (Snozzi & Crofts, 1984). Antimycin virtually abolishes Q_i function in the millisecond time scale to prevent cyt b_H reoxidation and the oxidation of a second QH_2 at the Q_o site. The kinetics of QH_2 oxidation observed by monitoring ferricytochrome $c_1 + c_2$ reduction under these conditions is complicated by the presence of the 2Fe2S center (Bowyer et al., 1980). However, in the uninhibited state, the time course of reduction of ferricyt $c_1 + c_2$ is a useful guide for the oxidation of the second QH_2 at the Q_o site, completing the catalytic cycle of the cyt bc_1.

Oxidation of QH_2 at the Q_i Site. QH_2 oxidation at the Q_i site was determined by observing cyt b_H reduction under conditions when the Q_o site function is inhibited by myxothiazol or stigmatellin. It has been shown with *Rhodobacter* that at high pH (Glaser et al., 1984; Robertson et al., 1984) or low [Q_{pool}] (Robertson et al., 1984) flash-activated cyt b_H reduction can occur through the Q_i site in a reaction that proceeds in the reverse of the physiological direction, as shown:

$$Q_iH_2 + \text{ferricyt } b_H \leftrightarrow Q_i^- + \text{ferrocyt } b_H + 2H^+ \quad (2)$$

Inhibitor Titrations of Mutants. The cyt *b* reduction experiment with antimycin present (i.e., cyt b_H reduction via Q_o) was also used to assay, in vitro, the sensitivities of the mutants to inhibitors. In this assay chromatophores from each mutant were poised at an E_h of approximately 240 mV so that the Q_{pool} was completely oxidized prior to activation. After the flash, approximately one QH_2 enters the Q_{pool} per cyt bc_1 complex, and its oxidation by the Q_o site was measured by cytochrome b_H reduction in the presence of antimycin to block Q_i function as described above. The rate of cyt b_H reduction as a function of inhibitor concentration was essentially constant so that the inhibition of Q_o could be monitored simply by the extent of cyt b_H reduction 50 ms after the flash. The I_{50} values reported represent the cuvette concentration of added inhibitor. Each mutant was assayed with myxothiazol and stigmatellin as well as with UHDBT. Although mutants resistant to mucidin were selected, the unavailability of this inhibitor prevented assay of its effect on cyt b_H reduction.

Chemicals. *N*-Methyldibenzopyrazine methylsulfate (PMS), *N*-ethyldibenzopyrazine ethosulfate (PES), antimycin, and Good buffers were purchased from Sigma. Myxothiazol was purchased from Boehringer-Mannheim Biochemicals. UHDBT was obtained from Dr. B. L. Trumpower, Dartmouth University, and stigmatellin was a generous gift of Dr. G. Höfle, Gesellschaft fur Biotechnologische, Braunschweig. Quinhydrone, 2-hydroxy-1,4-naphthoquinone (OHNQ), and 2,3,5,6-tetramethyl-*p*-phenylenediamine (DAD) were obtained from Aldrich. Pyocyanine was synthesized by photooxidation of PMS and subsequently purified by chloroform extraction. All other chemicals were reagent grade and were purchased from commercial sources.

Results

Table I details the phenotypes and amino acid substitutions for each of the seven inhibitor-resistant mutants studied as well as for mutant R126 (G158D). Five of the amino acid replacements fall between positions M140 and T163, spanning the G158D substitution, while the other two, L106 and V333, are at considerable distances in the primary sequence from this region. In the process of collecting inhibitor-resistant

mutants about 50 were isolated (Daldal et al., 1989). However, and quite remarkably, the acquisition of resistance due to substitutions mapping in *fbc* (*pet*) was restricted to only six residues, and of these six positions only one was substituted with more than one (i.e., F144S,L) alternative residue. The chromatophore preparations of each mutant were examined in the same way as was the G158D mutant (Robertson et al., 1986) and were found to possess RC and cyt bc_1 complements at concentrations similar to those for MT1131, the strain containing the wild-type cyt bc_1. Moreover, there appeared to be no differences in the assembly, degradation, or overall integrity of the RC–Q_{pool}–cyt bc_1–cyt c_2 cyclic electron-transfer system (data not shown).

In Vitro Inhibitor Sensitivity of Mutants. Table I shows I_{50} values calculated for the effect of myxothiazol, stigmatellin, and UHDBT on the extent of cyt b_H reduction via Q_o. Each mutant exhibits a general pattern of inhibition of cyt bc_1 activity that parallels the effects of stigmatellin and myxothiazol on the rate of growth of each strain (Daldal et al., 1989). It is also clear that alterations in different amino acid residues confer different degrees of resistance. More specifically, F144L and F144S exhibit resistance to myxothiazol at concentrations about 500-fold higher than wild type while the remainder of the myxothiazol- or mucidin-resistant strains are resistant to 10-fold higher concentrations. M140I, F144L, T163A, and V333A exhibit stigmatellin resistance to concentrations more than 7-fold higher than that required for inhibition of wild type, and these strains also show resistance to UHDBT to levels around 3- to 5-fold that of the wild-type strain. Note that an effect of UHDBT on growth could not be measured and therefore UHDBT resistance could not be selected for (Daldal et al., 1989).

Kinetics of Cyt bc_1 Turnover in Inhibitor-Resistant Mutants. The kinetics of cyt bc_1 turnover were measured as a function of the redox state of the Q_{pool} with a view toward revealing the source of alterations in Q_o site function in different mutants.

(*a*) *Kinetics with the Q_{pool} Reduced before Activation.* Under these conditions, established before activation, there are approximately 50 QH_2/0 Q/cyt bc_1, conditions expected to yield maximal QH_2 oxidation rates following flash activation. Table I lists the rates of cyt bc_1 turnover (i.e., two QH_2 molecules oxidized at the Q_o site) measured by observing the rate of cyt $c_1 + c_2$ reduction after flash oxidation. Values are given for the seven inhibitor-resistant mutants, the dysfunctional G158D, and the wild-type strain, MT1131. The standard deviations presented reflect variations in chromatophore preparations from three to five different batches of cells. The rate of turnover in the wild-type strain is 362 ± 43 s^{-1} when Q_{pool} is reduced prior to activation. Mutants selected for stigmatellin resistance with substitutions M140I, T163A, and V333A, and yielding >7-fold weaker stigmatellin binding, display rates of QH_2 oxidation remarkably unaltered from the wild-type value. On the other hand, mutants selected for myxothiazol resistance with substitutions G152S, F144S, and F144L, giving 30-, 500-, and 500-fold decreased affinity, are slowed by 1.2-, 1.5-, and 12-fold. The only mutant selected for mucidin resistance (not measured in the chromatophores), L106P, displayed a 4.4-fold slowing in turnover.

(*b*) *Kinetics with the Q_{pool} Oxidized before Activation.* These conditions, where approximately one QH_2/cyt bc_1 is introduced into the oxidized Q_{pool} (1 QH_2/50 Q/cyt bc_1) after flash activation, yield a minimum rate for turnover (Prince et al., 1978; Crofts et al., 1983). Table I shows that the flash-induced rate of ferricyt $c_1 + c_2$ reduction measured for

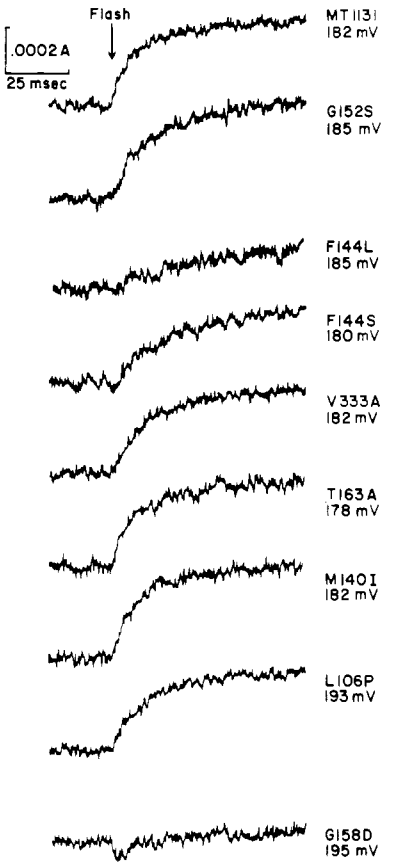

FIGURE 2: Kinetics of Q_o-mediated cyt b_H reduction. Conditions were as outlined in Figure 1 except that antimycin was added to a final concentration of 5 μM. The redox potential was set between 180 and 200 mV, i.e., with Q_{pool} fully oxidized.

wild type is approximately 18 s^{-1}, some 20-fold slower than the rate observed when Q_{pool} is fully reduced before activation. Kinetics observed for the mutants generally follow the same hierarchy as was seen when Q_{pool} was reduced before activation. However, the reliability of measurements under these conditions was lower, due to greater variations (see Table I) in the rate of cyt $c_1 + c_2$ reduction encountered from one chromatophore preparation to another. Also, it must be stressed that two QH_2 must be oxidized to yield a complete turnover and under Q_{pool}-oxidized conditions the rate is limited by the availability of substrate, i.e., QH_2 is subsaturating (Matsuura et al., 1983b; Crofts et al., 1983).

Under Q_{pool}-oxidized conditions, a reliable measure of a single QH_2 oxidation at the Q_o site rate is afforded by observation of cyt b_H reduction in a cyclic system whose complete turnover is inhibited by antimycin (see Materials and Methods). Figure 2 shows representative traces of cyt b_H reduction with chromatophores poised under these conditions. The measured rates are again listed in Table I. Mutants V333A, T163A, and M140I, selected for stigmatellin resistance, exhibit little if any deviation in rate from wild-type MT1131. The mutants selected for myxothiazol resistance, G152S, F144S, and F144L, on the other hand, have rates 1.3-, 1.8-, and 17.8-fold slower than wild type, respectively, while L106P selected for mucidin resistance has a rate 1.8-fold slower than wild type. In mutant G158D, there is no discernible reduction of cyt b_H on the time scale used for these experiments (Robertson et al., 1986). Thus, the cyt b_H reduction data confirm that the mutations cause a roughly proportional slowing of QH_2 oxidation independent of whether the Q_{pool} is reduced or oxidized. An intriguing exception is L106P, whose cyt bc_1 turnover rate (i.e., two QH_2 oxidized at Q_o) is lowered 5-fold

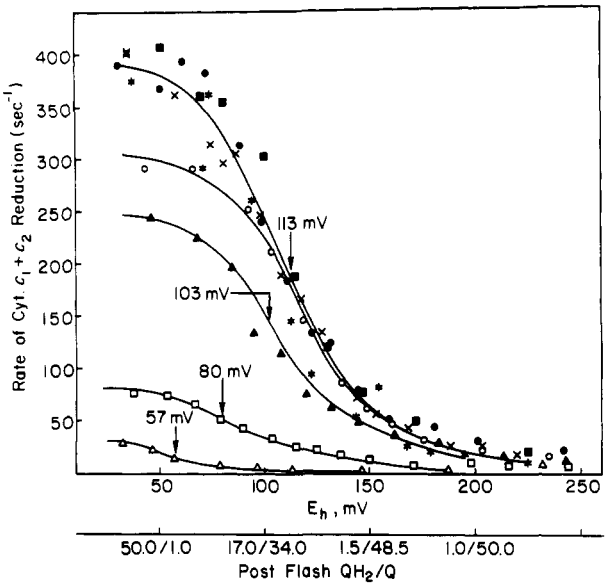

FIGURE 3: Redox potential dependence of cyt c_1 + c_2 reduction following flash delivery. Chromatophores were suspended in 50 mM MOPS and 100 mM KCl, pH 7.0. The final concentration of RC in the cuvette was 0.11 μM. PMS, PES, and pyocyanine were added to 1 μM, DAD to 2.5 μM, and OHNQ to 5 μM. Valinomycin was added to a final concentration of 3 μM. The redox potential was varied by addition of sodium dithionite and potassium ferricyanide. Data were obtained and analyzed as outlined under Materials and Methods. Experiments were performed on at least three chromatophore preparations, and the standard deviation for the maximum rate, i.e., with Q_{pool} fully reduced, was calculated for each strain. The average maximum and minimum values found are listed in Table I. Symbols: (●) wild type; (○) G152S; (△) F144L; (▲) F144S; (*) M140I; (■) T163A; (□) L106P; (×) V333A.

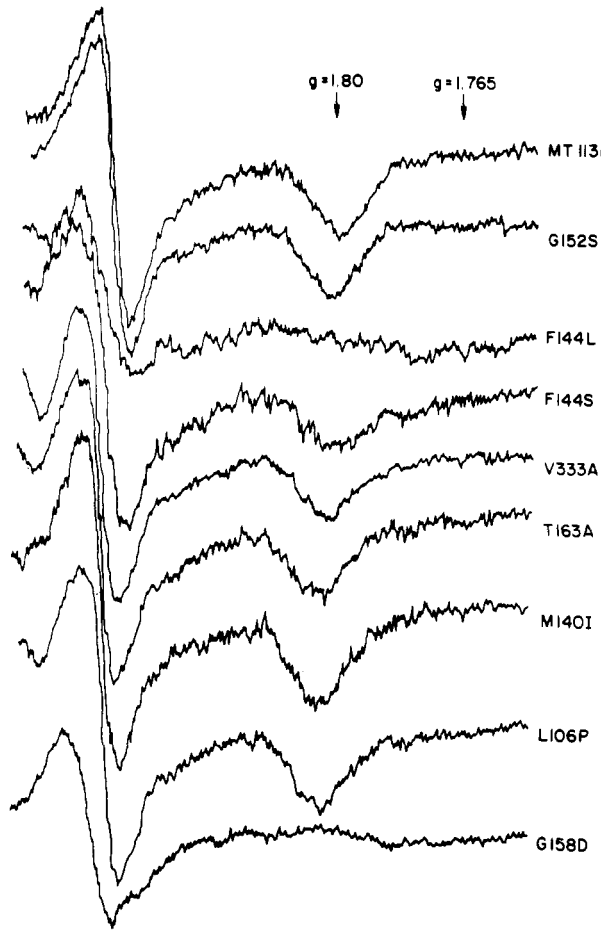

FIGURE 4: EPR spectra showing g_y and g_x features of the 2Fe2S center of mutant and wild-type strains. Chromatophores were suspended to a final RC concentration of 10 μM in 50 mM MOPS and 100 mM KCl, pH 7.0. PMS was added to 0.2 μM and sodium ascorbate to 20 mM. After 2-min incubation, samples were placed in quartz EPR tubes and frozen rapidly in 5:1 isopentane/methylcyclohexane equilibrated with liquid nitrogen. With the Q_{pool} reduced, all mutants showed the familiar broadened spectrum of the reduced 2Fe2S center (data not shown).

while its QH_2 oxidation rate (one QH_2 oxidized) is lowered less than 2-fold.

(*c*) *Dependency of the Rate of Cyt bc_1 Turnover on the QH_2/Q Ratio in Q_{pool}.* Figure 3 describes, using redox potentiometry, how the turnover rate changes as a function of the QH_2/Q ratio in Q_{pool}, measuring the rate of flash-oxidized cyt c_1 + c_2 reduction; again this was done for each of the mutants. It is clear from the set of titrations that the mutants selected for stigmatellin resistance are similar to the wild-type cyt bc_1, while the mutants selected for myxothiazol/mucidin resistance display distinctly modified dependencies of QH_2 oxidation rates as a function of the QH_2/Q ratio. It is also clear in the myxothiazol/mucidin resistant mutants, whose rates for this process are slowed, that the redox potential value at which the cyt c_1 + c_2 reduction rate is half-maximal is also lowered. For example, the value measured for wild type and for the strains selected for stigmatellin resistance is 113 mV while for L106P (5-fold slower than wild type), selected for mucidin resistance, and for the F144L (12.9-fold slower), selected for myxothiazol resistance, the values are 80 and 57 mV, respectively.

Binding of Q to Q_o: Observation of the 2Fe2S EPR Line Shape. The sensitivity of the EPR spectrum of the reduced 2Fe2S to the presence of Q in the Q_o site affords a means to examine the cyt bc_1 for any weakened binding of Q in the site in each of the mutants. Figure 4 shows the 2Fe2S EPR spectrum for the wild type and the mutants when the Q_{pool} was oxidized. The spectrum of the wild type (top trace) shows the well-known narrowed line shape at g = 1.80 that is exhibited by the reduced 2Fe2S when a Q is associated with the Q_o site. Similar spectra were displayed by all mutants with the exception of F144L and G158D; F144S also showed a consistently diminished g = 1.80 signal amplitude and the appearance of the broadened signal at higher field strengths.

Thus, mutants with modest or no impairment of QH_2 oxidation rates (WT and the stigmatellin-resistant M140I, T163A, and V333A) also exhibit similar narrowed g = 1.80 features indicative of a normal Q occupancy of the Q_o site. At the other extreme, F144L and G158D, mutants with the slowest rates of QH_2 oxidation at the Q_o site (12- and >100-fold slower than wild type), showed no narrow signal. We interpret this as suggesting that a parallel loss in the binding affinity for Q is incurred and that, in these mutants, Q does not occupy the Q_o site even under conditions when the Q_{pool} is fully oxidized. The F144S is intermediate to these extremes, appearing to possess a Q_o site that is partially occupied when the Q_{pool} is oxidized. Thus, it is worth considering that the loss of narrowing by Q and slowed cyt bc_1 turnover or QH_2 oxidation rates arise simply from a diminished binding strength of both Q and QH_2 at the Q_o site.

QH_2 Oxidation at Q_i. Experiments were performed on each of the inhibitor-resistant mutants to check whether the mutation that rendered the Q_o resistant to inhibitors had any effects on the function of Q_i. This was done in the presence of sufficient myxothiazol to inhibit Q_o function in the resistant strains. Flash-activated cyt b_H reduction was examined for alterations in amplitude, rate, and redox potential dependency. The kinetic traces in Figure 5 show that, with the exception

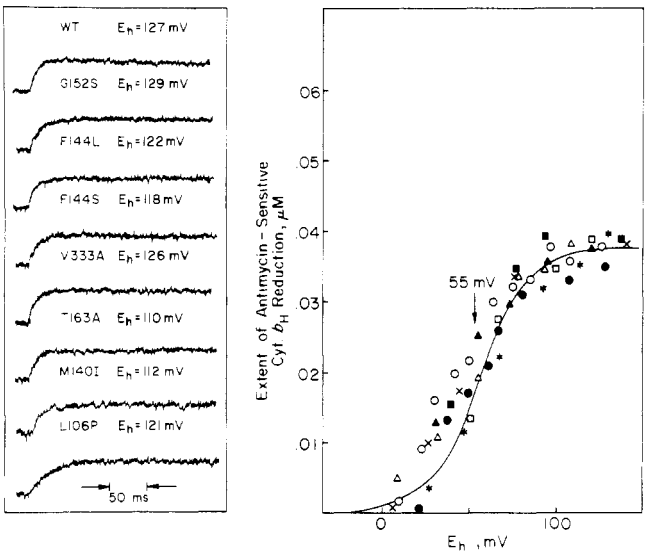

FIGURE 5: Cyt b_H reduction via site Q_i; kinetics, extent, and E_m for inhibitor-resistant mutants. Conditions were as outlined in Figure 2 except that myxothiazol was added (3 μM final or 25 μM final for myxothiazol-resistant mutants) instead of antimycin and the pH was buffered at 9.0 with 50 mM glycine. Symbols: (●) wild type; (○) F144S; (▲) F144L; (△) V333A; (*) G152S; (■) T163A; (□) L106P; (×) M140I.

of L106P, the mutants displayed very similar amplitudes and rates, which are listed in Table I. The response of the R126 (G158D) strain, also unaltered from the wild type, may be seen in Robertson et al. (1986). All strains displayed a similar antimycin sensitivity (data not shown). Additionally, all mutants show a similar trend of the extent of cyt b_H reduction as a function of redox potential with an E_{m9} value of 55 mV, in good agreement with Glaser and Crofts (1984) and Robertson et al. (1984). The exception, L106P, consistently exhibited a rate approximately 45% lower than the mean value measured for the remainder of the mutants and the wild-type strain. While this is not a drastic reduction in rate, it is of some interest, since it is the only example of an inhibitor-resistant mutation affecting the rates of QH_2 oxidation and cyt b_H reduction via both Q_o and Q_i.

Discussion

Selection of Mutants/Relationship to Functional Consequences. The high-affinity, site-specific natural product inhibitors of cyt bc_1 have been used for the study of individual redox reactions or partial turnovers and have led the way, in large part, to the present state of knowledge of the mechanism of the complex. In a different stratagem aimed at detailed understanding of its structure, a number of investigators have adopted the approach of inhibitor-resistant mutant selection followed by protein sequence determination. Besides bacteria, residue alterations giving resistance to Q_o site inhibitors have been identified in *Saccharomyces cerevisiae* (diRago et al., 1989) and to Q_i site inhibitors in *S. cerevisiae* (diRago et al., 1986; diRago & Colson, 1988) and *Schizosaccharomyces pombe* (Weber & Wolf, 1988). Specific resistance to a number of Q_o and Q_i inhibitors due to single amino acid substitutions has also been described in mutant strains of a mouse tumor cell line (Howell et al., 1987; Howell & Gilbert, 1987, 1988). The study presented here has attempted to draw on the advantages afforded by both strategies.

The inhibitor-resistant strains used in the present functional analysis were isolated as spontaneous Ps^+ mutants selected for resistance to one or more inhibitors of ubiquinol oxidation at the Q_o site of the cyt bc_1 complex (Daldal et al., 1989). The selection procedure is designed to yield photosynthetically competent (Ps^+) mutants. The amino acid substitutions conferring resistance, therefore, are those that allow the organism to tolerate the presence of the inhibitors while minimizing deleterious effects on function. Mutants with drastic functional alterations may be missed due to a failure to form discernible colonies during the time of selection. The limits of slowing of Q_o site catalyzed QH_2 oxidation tolerated by the bacteria growing under laboratory conditions in the presence of inhibitor appear to be somewhere in the region of 10- to 20-fold slower than those of the wild-type strain. The F144L mutant, having a turnover rate approximately 20-fold slower than wild type, was most severely affected, possibly placing this strain near a limit below which growth would not be detected.

The appearance of a given kind of spontaneous inhibitor-resistant mutant in the selection procedure is a function of the frequency of base substitution to code for alternate residues and may be limited by the above-mentioned practical considerations to those residues allowed by single base codon substitutions. For example, given the codon usage of the *fbc* (*pet*) operon and the G/C-rich usage in the third position of the codons in *R. capsulatus* (Davidson & Daldal, 1987a), there are only six possible single base pair substitutions that may be observed at F144: L, S, I, Y, V, and C. Apparently, only the substitution of L (for stigmatellin and myxothiazol) or S (for myxothiazol) meets the criterion of maximal inhibitor resistance versus the tolerable loss of QH_2 affinity. Work in progress has shown that strains constructed with L, S, I, Y, V, and C at residue 144 have functional cyt bc_1 (Ding, Robertson, Tokito, Daldal, and Dutton, unpublished results).

Subunit Location of Inhibitor-Resistant Residue Substitutions. It may seem unusual that all mutants isolated were in the cyt *b* polypeptide (Daldal et al., 1989), especially in view of the history of effects on the 2Fe2S cofactor by compounds interacting with the Q_o site. These effects include not only EPR line-shape changes induced by ubiquinone and inhibitor interactions with the Q_o site but also substantial (0.1–0.3-V) midpoint shifts induced by inhibitors. Especially relevant is the observation of Matsuura et al. (1983a), who demonstrated that the binding of UHDBT at the Q_o site was changed at least 20-fold, dependent upon the redox state of the 2Fe2S, i.e., UHDBT binds more tightly to the reduced form of 2Fe2S. Clearly, the 2Fe2S cofactor is energetically strongly coupled to events occurring in the Q_o site.

Brandt et al. (1988) have presented data which show that certain methoxyacrylate inhibitors (myxothiazol and mucidin) bind to cyt bc_1 devoid of the FeS subunit. Thus, while the 2Fe2S center reports inhibitor and ubiquinone binding at the Q_o site, it may not supply amino acid side-chain determinants to Q_o. Alternatively, if there are pertinent inhibitor binding residues in the 2Fe2S subunit, alteration of these residues may be impossible without (a) leading to Q_o function at a level below the threshold that allows photosynthetic growth in the laboratory or (b) leading to failure to assemble the 2Fe2S cluster or the cyt bc_1 complex. Whatever the reason for the absence of inhibitor-resistant mutations in the FeS subunit, it is clear that the cluster interacts strongly and locally with the Q_o site occupant.

Location of Mutations in the Low-Dielectric Medium of the Membrane. It is valuable to examine the sequence changes responsible for the mutant phenotypes with respect to the predicted secondary structure (Saraste, 1984; Widger et al., 1984) as recently modified by several groups (Rao & Argos, 1986; Crofts et al., 1988; Howell & Gilbert, 1988; Brasseur, 1988). Figure 6 shows eight transmembrane helical segments

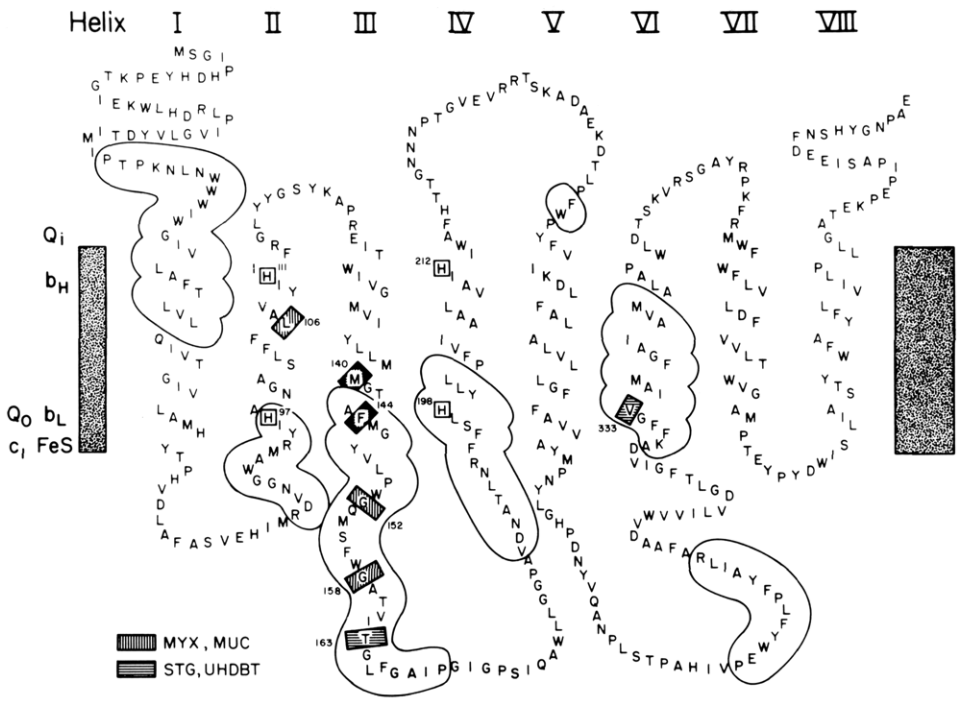

FIGURE 6: Amino acid sequence of cyt *b* showing membrane-penetrating helices. The folding pattern is taken from Rao and Argos (1986), Crofts et al. (1987), and Howell and Gilbert (1987). The sequence linking helices III and IV, though not shown as such, is postulated by these authors to be an amphipathic helix arranged at the edge of the membrane. Areas shown in outline are stretches of sequence with strong chemical homology over cyt *b* sequences from a number of phylogenetically diverse species (Howell, 1989). Contained in blocks with appropriate hatching to indicate resistance to myxothiazol or stigmatellin are residues altered to give inhibitor resistance. Those residues whose alterations result in cross-resistance are hatched in both patterns.

with the four cyt bc_1 invariant histidines (i.e., H97, H111, H198, and H212) thought to be ligands for the two *b*-type cytochromes. Also, shown in outline are areas of sequence conservation derived from an in-depth examination of cyt *b* sequences over a broad phylogenetic range (Howell, 1989) The six amino acid substitutions giving inhibitor-resistant phenotypes, as well as that responsible for the R126 phenotype at G158, are in three regions of the cyt *b* sequence [see also Daldal et al. (1989)]. Five of the mutants are located in a loop between helices III and IV, a region that also contains the lethal G158D. V333 in helix VI is quite distant in the sequence from this group. Likewise, L106 is separate, located in helix II between two (H97 and H111) of the four histidine ligands to the cyt *b* hemes (Hauska et al., 1988).

With the exception of residue L106, all the mutant positions are located in or near relatively invariant regions of the cyt *b* sequence (Howell, 1989) and are placed well toward the periplasmic, cytochrome *c* side of the membrane. Thus, their positioning is consistent with the proposed location of the Q_o site in the membrane profile from functional studies. Moreover, they are in proximity to the 2Fe2S center and cyt b_L (see Figure 1). As such, this supports the idea that the effects of ubiquinone and inhibitor binding at the Q_o site on the 2Fe2S EPR line shape and E_m value arise from changes in local forces rather than from more global alterations in protein structure.

It is worth noting that six of the mutations yield altered inhibitor binding and/or impaired function at Q_o without any effects on QH_2 oxidation at the Q_i site. This substantiates the idea that the two ubiquinone binding sites are distant from one another and apparently do not overlap [see also Robertson et al. (1986) and Robertson and Dutton (1988)].

The single exception to the above generalities is L106P, which has a small, but significant, effect on the oxidation rate of QH_2 at both sites (as measured in the presence of antimycin or myxothiazol). However, L106 is also exceptional in its location (Figure 6). It is not close to a region of structural invariance (Howell, 1989) and maps far from the outside surface of the membrane between two of the invariant histidine ligands of the cyt *b* hemes, H97 and H111. As such, it is located roughly equidistant from the proposed positions of the Q_o and Q_i sites. Thus, this mutation cannot be regarded as one located in the Q_o region generally defined by the other six mutants. The L106 alteration to proline, a residue known to be stereochemically incompatible with helix formation [see Creighton (1984)], may impair QH_2 oxidation by transmitting deleterious structural alterations to both Q binding sites or, alternatively, to the closer histidines ligating one or both cyt *b* hemes. In fact, if the mutation affects cyt b_H, we may explain the discrepancy between the rates for turnover (i.e., two QH_2 oxidations assayed by cyt $c_1 + c_2$ reduction; antimycin present) vs those for a single QH_2 oxidation via Q_o (cyt b_H reduction) in L106P (Table I) by assuming that it is the cyt b_H interaction with Q_i that is affected.

Interaction of the Q and QH_2 from Q_{pool} with the Q_o Site. Detailed experimental information is lacking on the kinetics and binding affinities of Q and QH_2 for the Q_o site though indirect evidence is available. If we combine the kinetics and the 2Fe2S line-shape analysis reported here with results of earlier studies, a semiquantitative picture emerges. Matsuura et al. (1983a) using *R. sphaeroides* chromatophores showed that the $g = 1.80$ EPR feature of the 2Fe2S, reporting Q occupancy of Q_o, remained fully formed as the Q_{pool}/cyt bc_1 ratio was decreased by ubiquinone extraction by 85%; this decrease is equivalent to a change from 30 to approximately 4 Q/RC[2] or, as estimated by Ding, Robertson, and Dutton (unpublished results), from 50 to 6 Q/cyt bc_1. However, further extraction to a level of 1.9 Q/RC (or 2–3 Q/cyt bc_1) nearly eliminated the $g = 1.80$ signal. This suggested that the Q from Q_{pool} has a high affinity for the site. Moreover, redox

[2] The quantitation of Q was referenced to the RC concentration in Matsuura et al. (1983a).

titrations of the $g = 1.80$ signal amplitude followed the Q_{pool} Nernst curve, which suggested that the affinity of QH_2 for the site equals that of Q. Very strong support for this conclusion was provided by inhibitor titrations performed when the Q_{pool} was all Q or all QH_2; under each condition the I_{50} for UHNQ was the same (Matsuura et al., 1983a). These data suggest that in native membranes the Q_o site is essentially fully occupied either by Q or by QH_2. Very recent work with *R. capsulatus* (Ding, Robertson, Daldal, and Dutton, unpublished results) has yielded similar conclusions and has clarified matters considerably regarding the 2Fe2S signal response to Q_o site occupancy (see Added in Proof).

With this view of the Q_o site–Q_{pool} interaction, the rate of QH_2 oxidation in chromatophores may be governed by a combination of QH_2 concentration (substrate) and the competing presence of Q in the site (inhibitor), the exchange rates, k_{on} and k_{off}, for both Q and QH_2, and the internal rates of electron transfer within the catalytic sequence. Thus, the effects of the mutations on QH_2 oxidation may be understood as follows: Alteration of V333A, T163A, and M140I (STG^R) has no discernible effect on either binding of Q ($g = 1.80$ signal is the same as that of the wild type) or the binding and oxidation of QH_2 (the oxidation rate vs QH_2/Q ratio is the same as that of the wild type; Figure 3); in all cases, the redox potential at which the rate is half-maximal is higher than that of the Q_{pool} (113 mV vs 90 mV), showing that the maximum rate is attained when the Q_{pool} is only partly reduced prior to activation (approximately 7 QH_2/43 Q). This maximum rate is interpreted as reflecting internal rate restrictions governed by one or more of the subsequent electron-transfer or protolytic steps.

At the other extreme, the F144L displays loss of the $g = 1.80$ signal and gain in the broader g_x feature similar to that seen in the Ps^- G158D, indicative of an empty Q_o site even at 50 Q/cyt bc_1. Thus, for the two mutants F144S and F144L it is clear that there is a major loss of affinity of the site for Q. The loss of kinetic competency in the QH_2 oxidation rate is most simply explained by a parallel loss in the binding affinity of the site for QH_2. Hence, in the case of F144L a nearly fully reduced Q_{pool} is required to observe a measurable increase in rate of turnover; here the potential at which the rate is half-maximal is 57 mV (approximately 47 QH_2/3 Q). Hence, lowering the potential to establish 50 QH_2/0 Q has little effect; even at the maximum the rate is 15-fold slower than the rate of the wild type. In the case of G158D, even with a fully reduced Q_{pool} the rate was $\gg$100-fold slower.

The other F144 mutant (F144S) shows a partially diminished $g = 1.80$ signal when Q_{pool} is fully oxidized (Figure 4), indicating that this mutant has suffered a sufficient loss of affinity so that the site is only partially occupied at 0 QH_2/50 Q. In this mutant, the potential at half-maximal rate (Figure 3) is also lowered compared to the wild type, suggestive of weakened QH_2 binding although additional kinetic defects at other steps in the catalytic sequence cannot be ruled out.

Additional observations and conclusions related to the residue substitutions in these mutants are compiled in Table II.

Suggestions for Structural Modeling of the Q_o Site: Analogies to the Q_A and Q_B Sites of the Photosynthetic Reaction Center. Using the three-dimensional reaction center structures for *Rhodopseudomonas (Rps.) viridis* (Deisenhofer et al., 1985) and *R. sphaeroides* (Chang et al., 1986; Allen et al., 1988), we have explored the idea that ubiquinone binding sites may have some common structural features. We draw on the structures of Q_A and Q_B and the data regarding the binding of ubiquinone (to Q_A and Q_B) and of certain herbicide inhibitors (to Q_B). The generalizations that emerge, considered together with the spectroscopic, mutational, and functional observations reported here for the Q_o site, have been used to construct a hypothetical Q_o site as shown in Figure 7. Figure 7 also shows, for comparison, the structural elements of Q_A (panel A) and Q_B (panel B) and a map of myxothiazol and stigmatellin binding regions in Q_o (panel D). The evidence for this model is detailed as follows:

(1) Q_A and Q_B Site Structures. The sequences for the RC subunits of four purple, non-sulfur bacteria [*R. sphaeroides*, Williams et al. (1986); *R. capsulatus*, Youvan et al. (1984); *Rhodospirillum rubrum*, Belanger et al. (1988); *Rps. viridis*, Michel et al. (1986b)] have been determined and compared within the framework of the three-dimensional X-ray crystal structures for *Rps. viridis* and *R. sphaeroides* [see Komiya et al. (1988)]. The Q_A and Q_B sites each have an invariant histidine (HisM219[3] in Q_A and HisL190 in Q_B) which ligates Fe and possibly hydrogen bonds to the ubiquinone. Each site also has an aromatic residue roughly cofacially oriented with ubiquinone (Trp M252 in Q_A and Phe L216 in Q_B) and an aliphatic moiety on the opposite side of the ubiquinone ring [Val(or Leu)M226 in Q_A and Ile(or Val)L229 in Q_B]. Within each site is an invariant, nonionic polar side chain which is a candidate for hydrogen bonding to ubiquinone (ThrM222 in Q_A and SerL223 in Q_B) and a small nonpolar aliphatic residue (AlaM260 in Q_A and GlyL225 in Q_B). Additionally, there are invariant residues which do not provide structural determinants for ubiquinone binding by van der Waals contacts but are necessary for the tertiary site structure; for example, TyrL222 near site Q_B is shown in Figure 7B. The Q_A and Q_B site functions, though different in details of protonation, electrochemical midpoints, stabilization of semiquinone, etc., are similar with regard to the chemistry of their Q and QH_2 binding determinants [Q_A, Warncke and Dutton, unpublished results; Q_B, Rutherford and Evans (1980)] and may differ materially only in their surrounding residues whose role is not primarily structural. The immediate binding determinants may provide the chemical architecture for any ubiquinone binding site, and as such, these generalities have been assumed to operate at Q_o.

(2) Analogy to the Q_B Site Herbicide-Resistant Mutants in the Photosynthetic RC. The model proposes that the five residues determining inhibitor resistance (with the exception of L106) and the G158 residue are structural elements of the Q_o site. This tenet of the model is based partially upon the arguments outlined above as well as upon analogous inhibitor-resistance work done on the Q_B site of *Rps. viridis* (Sinning et al., 1990) and *R. sphaeroides* (Paddock et al., 1987) reaction centers. Three-dimensional structures for the Q_B site with ubiquinone bound for *R. sphaeroides* (Komiya et al., 1988) and with ubiquinone and the inhibitors *o*-phenanthroline and terbutryn for *Rps. viridis* (Michel et al., 1986a) have been solved from X-ray crystallographic data. These results show that residues altered to confer herbicide resistance are involved directly with Q binding at the site (PheL216, SerL223, IleL229) or, if indirectly involved (e.g., TyrL222), are within 6 Å of the ubiquinone.

(3) Q_o Site Structure. As pointed out in Davidson and Daldal (1987b), at least some of the residues altered to give inhibitor resistance in the Q_o site are similar to those conferring

[3] RC residues are numbered according to convention where the amino acid name is followed by the subunit name and the residue's numbered position in the sequence of that subunit. The numbers used are those for *R. sphaeroides* (Komiya et al., 1988).

Table II

selection	phenotype	sub-stitution	observation[h]	implications and interpretations for quinone catalysis	inhibitor action
none (wt)	MYX^S, STG^S, MUC^S	–	–	–	–
myxothiazol	MYX^R, STG^S, MUC^R	G152S	no detected Q and QH_2 weakening; little or no slowing in QH_2 oxidation; myx weakened by >2 kcal;[a,b] stig unaffected	G to S size increase and OH addition, minor effects	G to S size increase or OH addition weakens myx and muc; no consequence for stig
myxothiazol	MYX^R, STG^R, MUC^S	F144L	Q and QH_2 weakened by >1 kcal;[c] QH_2 oxidation slowed 20-fold; myx weakened by >3.6 kcal; stig weakened by >0.7 kcal	F to L aromatic to aliphatic or steric change deleterious; see also F144S below	F to L aromatic to aliphatic or steric change weakens myx and stig; no consequence for muc
myxothiazol	MYX^R, STG^S, MUC^S	F144S	Q and QH_2 binding weakened by 0.05–1 kcal; QH_2 oxidation slowed by <2-fold; myx weakened by >3.6 kcal; stig unaffected	F to S aromatic to aliphatic, OH addition, or size change deleterious, though less than F144L; OH curves L substitution; note: similar F to S in Q_B weakens terbutryn and *o*-phenanthroline[d]	F to S aromatic to aliphatic, OH addition, or size change weakens myx; OH ameliorates L with regard to stig resistance
mucidin	MYX^R, STG^S, MUC^R	L106P	no detected Q or QH_2 weakening; little effect on first QH_2 oxidized; full cyt bc_1 turnover impaired; myx weakened by >1.4 kcal; stig weakened by >0.5 kcal	L to P, no consequence to QH_2 oxidation or Q binding; causes damaging structural changes near cyt b_H; possibly impairs b_H to Q_i electron transfer	L to P weakens muc and myx; no consequence for stig
stigmatellin	MYX^S, STG^R, MUC^S	V333A	no detected Q or QH_2 binding change; no effect on QH_2 oxidation; myx unaffected; stig weakened by 1.1 kcal	V to A size decrease, no consequence	V to A size decrease weakens stig; no consequence for myx and muc
stigmatellin	MYX^S, STG^R, MUC^S	T163A	no detected Q or QH_2 binding change; no effect on QH_2 oxidation; myx unaffected; stig weakened by 1.1 kcal	T to A size decrease and OH loss no consequence; note: S to A change in Q_B weakens terbutryn and *o*-phenanthroline[d]	T to A size decrease or loss of OH weakens stig; no consequence for myx and muc
stigmatellin	MYX^R, STG^R, MUC^S	M140I	no detected Q or QH_2 binding change; no effect on QH_2 oxidation; myx weakened by >2 kcal; stig weakened by >1.4 kcal	sulfur of M and M to I structure change, no consequence; note: in Q_A, MetM218 and MetM256 in *R. sphaeroides* are AlaM216 and LeuM254 in *Rps. viridis*;[e] see text	loss of sulfur on M or M to I structural change weakens myx and stig; no consequence for muc
R126 (Ps^- mutant)	Ps^-	G158D	Q and QH_2 binding weakened; no detected QH_2 oxidation; note: stig binding unaffected[g]	G to D size change or carboxyl addition deleterious	G to A in mouse yields myx resistance[f]

[a] All free energy values expressed in kcal/mol; for brevity "mol" has been eliminated. [b] Calculation based upon I_{50} values; all free energy differences are determined from the following approximation: $\Delta G = -RT \ln [I_{50}(\text{mutant}) - I_{50}(\text{wild type})]$. [c] An estimate based on the virtual loss of the $g = 1.80$ EPR signal. $\Delta G_0 = -RT \ln K_{eq}$; taking $g = 1.80$ as a guide, K_{eq} is changed by at least a factor of 5 upon disappearance of the signal. [d] Sinning et al., 1989. [e] Komiya et al., 1988. [f] Howell and Gilbert, 1988. [g] Robertson and Dutton, unpublished results. [h] Abbreviations: myx, myxothiazol; stig, stigmatellin; muc, mucidin.

herbicide resistance in the Q_B site; in each site, mutations lead to alterations in binding and kinetics in broadly the same range. For example, in the Q_o site, F144 (F144S, MYX^R; F144L, STG^R, MYX^R) may be analogous to PheL216 in the Q_B site (providing van der Waals contact with ubiquinone) which when substituted to Ser provides resistance to both terbutryn and *o*-phenanthroline with a decrement in the binding affinity of ubiquinone. Likewise, V333 may be analogous to the Q_B IleL219, on the other side of the bound ubiquinone. This residue, when altered to methionine to give herbicide resistance, has a similar effect. Our model suggests that F144 and V333 are analogous to these residues in function and in position relative to the bound ubiquinone in Q_o. Preliminary data on mutants with 14 substitutions at F144 support the role of an aromatic residue in Q and QH_2 binding (Ding, Robertson, Tokito, Daldal, and Dutton, unpublished results). Another hydrophobic residue such as I162, which alters to yield spontaneous inhibitor resistance in *S. cerevisiae* (di Rago et al., 1989), located between the residues 140 and 163, could serve a similar function to V333 and might easily be substituted in the site model.

Like Q_A and Q_B, the hypothetical Q_o site incorporates nonpolar aliphatics (G152 and G158) and a nonionic, polar residue (T163). Also, like Q_A, which has methionines (MetM218, MetM256) which appear to guide the ubiquinone tail, Q_o has a methionine (M140) which alters to give inhibitor resistance and, in the model, is suggested to serve the same purpose. Note that T163 in the Q_o model maps in the stigmatellin binding region but does not provide critical hydrogen bonding to ubiquinone carbonyl or phenoxy groups on Q or QH_2.

(*4*) *Helical Topology of the Cyt b Polypeptide.* The six residues of the site are found on three helical segments displaced within the primary structure of cyt *b*. To form a single region, therefore, helix II (containing L106 and the heme ligands H97 and H111), helix III (containing two inhibitor-binding residues, M140 and F144), the amphipathic helix between III and IV (with two inhibitor-binding residues, G152 and T163, and G158) and helix VI (with V333) have been brought into close proximity. The suppositions used to move these segments of structure close to each other are based in part upon the modeling of Brasseur (1988), who used a predictive method to determine the topological interrelationships between membrane buried α-helices of cyt *b* based upon the calculation of hydrophobic moments. In his arrangement, helices II and IV (providing ligands for the cyt *b* hemes) and helix III are arranged close to each other; helix VI is in close proximity to III and IV.

(*5*) *Topology of Residues on Helix III and the Amphipathic Segment Linking III and IV.* Daldal et al. (1989) have postulated that three of the residues conferring resistance or causing dysfunction are on the hydrophobic side of the am-

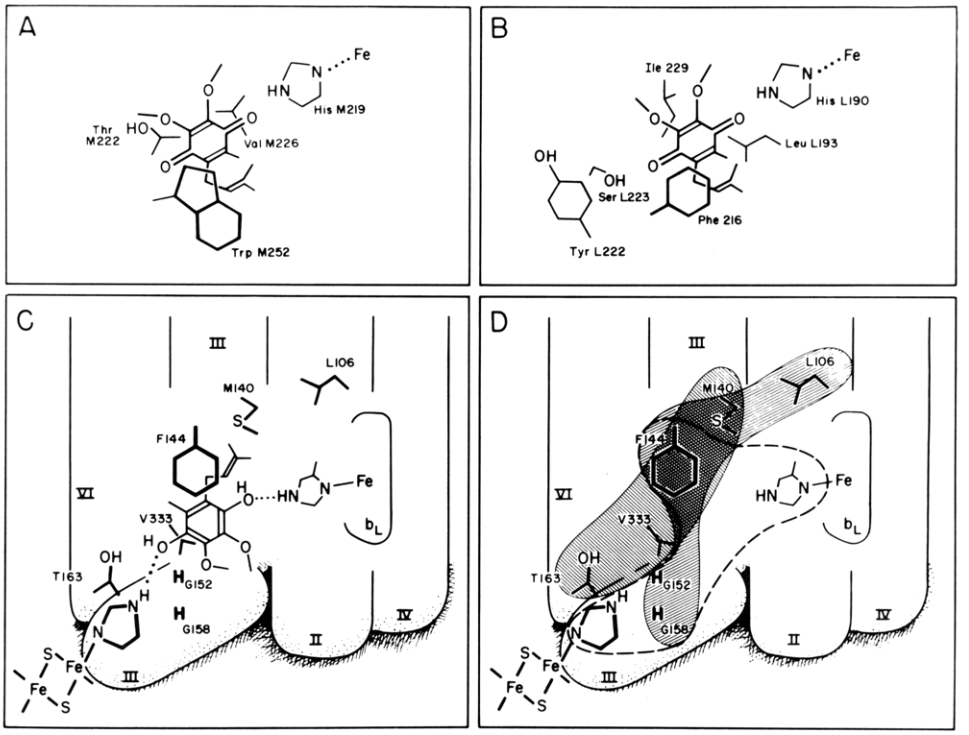

FIGURE 7: Structural model of the Q_o site. The model as presented has the α-helices organized to give an open view of the site. However, the model makes no predictions for these beyond providing the suggested spacial positioning to define the ubiquinone binding domain. Panel A: Three-dimensional model of Q_A of *R. sphaeroides*, showing residues surrounding the bound Q. This model is constructed from data in Michel et al. (1986a) and Komiya et al. (1988). Panel B: Three-dimensional model of the Q_B site showing residues near Q or residues altered to give herbicide resistance in *R. sphaeroides* (Paddock et al., 1986) and *Rps. viridis* (Sinning et al., 1989). Panel C: Hypothetical model of the Q_o site based upon analogies to Q_A and Q_B and upon the additional evidence outlined in the text. Panel D: Map of inhibitor binding regions within the Q_o site based upon the residues altered to give resistance to myxothiazol and/or stigmatellin. The dashed border encompasses the side chains critical for ubiquinone binding, the hatching surrounding T163, V333, F144, and M140 delineates the stigmatellin binding side chains, and the hatching around G158, G152, F144, M140, and L106 defines the myxothiazol or mucidin region.

phipathic, extramembranous segment of α-helix between helices III and IV. They have postulated that this portion of sequence is separated from helix III at a highly conserved proline near the membrane surface (P150; see their Figure 7). Helix III, moreover, contains two additional residues whose alterations result in resistance. A helical wheel analysis of helix III and the amphipathic segment shows that the residues which alter to give resistance may be brought into close proximity near the aqueous boundary of the cyt *b* polypeptide, but disposed toward the site interior.

(*6*) *Hydrogen Bonding to Histidines Ligating Fe in the Q_B and Q_A Sites.* We have speculated on the major hydrogen-bonding contacts to the carbonyls of the ubiquinone in Q_o, one involving either H97 or H198, proposed to be axial ligands to cyt b_L, and the other indirectly bonded to the 2Fe2S cofactor via a proposed histidine ligand of Rieske-type 2Fe2S centers (Cline et al., 1985; Powers et al., 1989; Gurbiel et al., 1989). This idea has also been proposed by Rich (1989). These suggestions are based on the following: (a) analogy to Q_A and Q_B, where both sites have been suggested to interact with their ubiquinone occupants through hydrogen bonds provided by histidines ligated to Fe; (b) the large number of reported E_m shifts (of the 2Fe2S) and spectral alterations (of the 2Fe2S and cyt b_L) induced by ubiquinone or inhibitor occupancy of Q_o (von Jagow & Link, 1986); (c) the nature of the catalytic event, a concerted action between 2Fe2S, cyt b_L, and QH_2/Q (Meinhardt & Crofts, 1983) which may be expected to be promoted by a strong overlap of wave functions; and (d) the effect of the 2Fe2S redox state on the affinity of the site for UHNQ and the reciprocal effect of the redox state of the UHNQ on the 2Fe2S spectrum and midpoint (Matsuura et al., 1983b). The indirect contact between the bound ubiquinone and an invariant histidine near to, but not ligating, the 2Fe2S center may be a reasonable alternative as postulated by Gatti et al. (1989).

(*7*) *Hydrogen Bonding from Protein Residues to Ubiquinone Carbonyl Oxygen Lone Pairs.* It is also suggested that the carbonyl(s) of Q and the phenoxyls of QH_2 interact with the site through similar linkages. Hence, in Figure 7D the phenoxyl and carbonyl oxygen lone pairs interact with hydrogen bond donors in a similar fashion with similar strength (Keske et al., 1990), thereby leading to similar binding affinities of Q and QH_2 for the site. Hence, any interactions occurring due to the phenoxyl hydrogen, if present in the site when comparing Q and QH_2, are predicted to sum to zero. A similar situation has been proposed to exist in the Q_B site where Q and QH_2 binding affinities are roughly similar (Rutherford & Evans, 1980; Wraight & Shopes, 1989). Obviously, and again as found in the Q_B site, the fate of the hydrogens/protons is crucial to the catalytic cycle of events. Rich (1987) has suggested that the preferred ubiquinol species bound to the Q_o site is the QH^- anion, and Robertson et al. (1983) have suggested that a proton exchange is associated with ubiquinone binding to the Q_i site. At this time, little more can be said concerning protonation/deprotonation and the reactions at the Q_o and Q_i sites.

It is important to stress that Figure 7 is a working model based upon functional data and indirect structural observations and is designed to provide a foundation for future experiments aimed at a precise description of the mechanism of Q_o. There are data that may contradict some details of this simple schematic representation, however. For example, analyses of evolutionary conservation within the sequence of cyt *b* (Howell, 1989) have shown regions of conservation other than those

utilized to construct the model. The extramembranous loop between helices V and VI, for example, containing the highly conserved PEW triplet has been postulated to be required for the Q_o site (Hauska et al., 1988). Also, Brandt et al. (1988) have presented binding and kinetic data for certain low-affinity methoxyacrylate inhibitors which imply that they bind near to but not coincident with the Q_o site. Though the model incorporates the idea that inhibitor and substrate side-chain determinants are not identical (Figure 7D), it remains to be seen whether partial overlap (as opposed to no overlap) of binding regions can explain the noncompetitive behavior. Experiments combining site-directed mutagenesis and various functional approaches are currently in progress which may support, amend, or invalidate the model.

Added in Proof

Recent work in this laboratory (H. Ding, D. E. Robertson, F. Daldal, and P. L. Dutton, unpublished results) has attempted to provide conclusive proof that the very broad EPR signal of the most severely affected mutants (e.g., F144L and G158D) is due to a Q_o site unoccupied by Q or QH_2, the result of a much-weakened Q_o site binding affinity. Experiments employing extraction and reconstitution of Q_{pool} from wild-type *R. capsulatus* have demonstrated the following: (a) that the complete removal of ubiquinone from Q_{pool} and the Q_o site reversibly produces a much-broadened spectrum of the 2Fe2S cluster, characterized by a diminished $g_y = 1.90$ signal and a shallow g_x feature at $g = 1.76$; (b) that this extracted spectrum is distinctly unlike those seen when the Q_{pool} is in the Q or QH_2 form, which show prominent transitions at $g = 1.80$ and 1.78, respectively, but is very similar to the dysfunctional mutants; (c) that Q and QH_2 bind to the Q_o site relatively tightly and nearly equally (half-occupied at 1.5–2 Q or QH_2/cyt bc_1 complex); and (d) that the Q_o site of mutants such as F144L or G158D must suffer a greater than 40-fold weakening in the affinity of Q and QH_2. Hence, our new results substantiate our previously held, but only indirectly supported, view that the *R. capsulatus* mutants severely affected in their ability to oxidize QH_2 possess Q_o sites with lowered affinity for Q and QH_2 in the Q_{pool}.

The above results allow observations made earlier by two groups working on the structure of the 2Fe2S center to be interpreted within the framework of the Q_o site model (Figure 7) as it applies to the occupied vs unoccupied site: (a) Romish et al. (1987) have reported the g values for the EPR spectrum of the isolated FeS subunit from *Neurospora crassa* to be $g_z = 2.03$, $g_y = 1.90$, and $g_x = 1.75$. The high-field shifted g_x value is similar to that observed with Q-extracted wild-type or severely affected mutant cyt bc_1 (Figure 4). The soluble subunit spectrum would be expected to mirror the situation wherein the Q_o site is unoccupied if ubiquinone does not bind to the 2Fe2S subunit when isolated. (b) Gatti et al. (1989) in their Figure 4 present EPR spectra for the 2Fe2S of a cyt bc_1 complex from *S. cerevisiae* in which a residue of the 2Fe2S subunit is mutated, and which is severely functionally impaired. The spectrum in this mutant (N705) is broadened beyond that seen in wild type when the Q_{pool} is oxidized or reduced (i.e., Q or QH_2 occupying the Q_c site) and is unaffected by the redox state of the Q_{pool}. Our interpretation of these spectra, in the light of the above-mentioned extraction studies, is that this mutation, engineered in the 2Fe2S subunit of cyt bc_1 complex, has produced a Q_o site that, like our cyt b polypeptide mutants (e.g., F144L, G158D), has a very much lowered affinity for Q and QH_2. Thus, although none of our inhibitor-resistant mutants resulted in 2Fe2S subunit residue substitutions, it is clear that these data indicate that there are residues in the 2Fe2S subunit which can affect the binding of ubiquinone at the Q_o site. Hence, further developments on the Q_o site structural model shown in Figure 7 can be expected to include more involvement of the 2Fe2S subunit residues.

Registry No. Ubiquinol–cytochrome c_2 oxidoreductase, 9027-03-6; stigmatellin, 91682-96-1; myxothiazol, 76706-55-3; mucidin, 52110-55-1.

References

Allen, J. P., Feher, G., Yeates, T. O., Komiya, H., & Rees, D. C. (1987) *Proc. Natl. Acad. Sci. U.S.A. 4*, 5730–5734.

Belanger, G., Berard, J., Corriveau, P., & Gingras, G. (1988) *J. Biol. Chem. 263*, 7632–7638.

Bevington, P. R. (1969) *Data Reduction and Error Analysis for the Physical Sciences*, pp 204–246, McGraw-Hill, New York, NY.

Bowyer, J. R., Dutton, P. L., Prince, R. C., & Crofts, A. R. (1980) *Biochim. Biophys. Acta 592*, 455–460.

Brandt, U., Schagger, H., & von Jagow, G. (1988) *Eur. J. Biochem. 173*, 499–506.

Brasseur, R. (1988) *J. Biol. Chem. 263*, 12571–12575.

Chang, C. H., Tiede, D., Tang, J., Smith, U., Norris, J., & Schiffer, M. (1986) *FEBS Lett. 205*, 82–86.

Cline, J. F., Hoffman, B. M., Mims, W. B., LaHaie, E., Ballou, D. P., & Fee, J. A. (1985) *J. Biol. Chem. 256*, 3251–3254.

Creighton, T. E. (1984) *Proteins*, p 315, W. H. Freeman and Co., New York, NY.

Crofts, A. R., & Wraight, C. (1983) *Biochim. Biophys. Acta 726*, 149–185.

Crofts, A. R., Meinhardt, S. W., Jones, K. R., & Snozzi, M. (1983) *Biochim. Biophys. Acta 723*, 202–218.

Crofts, A. R., Robinson, H., Andrews, K., van Doren, S., & Berry, E. (1987) in *Cytochrome Systems: Molecular Biology and Bioenergetics* (Papa, S., Chance, B., Ernster, L., & Jaz, J., Eds.) pp 617–624, Plenum Press, New York.

Daldal, F., Davidson, E., & Cheng, S. (1987) *J. Mol. Biol. 195*, 1–12.

Daldal, F., Tokito, M. K., Davidson, E., & Faham, M. (1989) *EMBO J. 8*, 3951–3961.

Davidson, E., & Daldal, F. (1987a) *J. Mol. Biol. 195*, 12–24.

Davidson, E., & Daldal, F. (1987b) *J. Mol. Biol. 195*, 25–29.

Deisenhofer, J., Epp, O., Miki, K., Huber, R., & Michel, H. (1985) *Nature (London) 318*, 618–624.

deVries, S., Albracht, S. P. J., & Leeuwerik, F. J. (1979) *Biochim. Biophys. Acta 546*, 316–333.

deVries, S., Albracht, S. P. J., Berden, J. A., & Slater, E. C. (1981) *J. Biol. Chem. 256*, 11996–11998.

diRago, J.-P., & Colson, A.-M. (1988) *J. Biol. Chem. 263*, 12564–12570.

diRago, J.-P., Perea, X., & Colson, A.-M. (1986) *FEBS Lett. 208*, 208–210.

di Rago, J.-P., Coppee, J.-Y., & Colson, A.-M. (1989) *J. Biol. Chem. 264*, 14543–14548.

Dutton, P. L. (1978) *Methods Enzymol. 54*, 411–435.

Dutton, P. L. (1986) in *Encyclopedia of Plant Physiology* (Staehlin, A., & Arntzen, C. J., Eds.) Vol. 19, Springer-Verlag, West Berlin.

Dutton, P. L., Petty, K. M., Bonner, H. S., & Morse, S. D. (1975) *Biochim. Biophys. Acta 387*, 536–556.

Gatti, L. D., Meinhardt, S. W., Ohnishi, T., & Tzagaloff, A. (1989) *J. Mol. Biol. 205*, 421–435.

Glaser, E., & Crofts, A. R. (1984) *Biochim. Biophys. Acta 766*, 322–333.

Glaser, E., Meinhardt, S. W., & Crofts, A. R. (1984) *FEBS Lett. 178*, 336–342.

Gurbiel, R. J., Batie, C. J., Sivaraja, M., True, A. E., Fee, J. A., Hoffman, B. M., & Ballou, D. P. (1989) *Biochemistry 28*, 4861–4871.

Hauska, G., Nitschke, W., & Herrmann, R. G. (1988) *J. Bioenerg. Biomembr. 20*, 211–228.

Howell, N. (1989) *J. Mol. Evol. 29*, 157–169.

Howell, N., & Gilbert, K. (1987) in *Cytochrome Systems: Molecular Biology and Bioenergetics* (Papa, S., Chance, B., Ernster, L., & Jaz, J., Eds.) pp 79–86, Plenum Press, New York.

Howell, N., & Gilbert, K. (1988) *J. Mol. Biol. 203*, 607–618.

Howell, N., Appel, J., Cook, J. P., Howell, B., & Houswirth, W. W. (1987) *J. Biol. Chem. 262*, 2411–2414.

Keske, J. M., Bruce, J. M., & Dutton, P. L. (1990) *Z. Naturforsch. 45C*, 430–435.

Komiya, H., Yeates, T. O., Rees, D. C., Allen, J. P., & Feher, G. (1988) *Proc. Natl. Acad. Sci. U.S.A. 85*, 9012–9016.

Konstantinov, A. A., & Popova, E. (1988) *Cytochrome Systems: Molecular Biology and Bioenergetics* (Papa, S., Chance, B., Ernster, L., & Jaz, J., Eds.) pp 751–765, Plenum Press, New York.

Matsuura, K., Bowyer, J. R., Ohnishi, T., & Dutton, P. L. (1983a) *J. Biol. Chem. 258*, 1571–1579.

Matsuura, K., O'Keefe, D. P., & Dutton, P. L. (1983b) *Biochim. Biophys. Acta 722*, 12–22.

Meinhardt, S. W., & Crofts, A. R. (1982) *FEBS Lett. 149*, 223–227.

Meinhardt, S. W., & Crofts, A. R. (1983) *Biochim. Biophys. Acta 723*, 219–230.

Michel, H., Epp, O., & Deisenhofer, J. (1986a) *EMBO J. 5*, 2445–2451.

Michel, H. Weyer, K. A., Gruenberg, H., Dunger, I., Oesterhelt, D., & Lottspeich, F. (1986b) *EMBO J. 5*, 1149–1158.

Mitchell, P. (1975) *FEBS Lett. 59*, 137–139.

Mitchell, P. (1976) *J. Theor. Biol. 62*, 327–367.

Moser, C. C., & Dutton, P. L. (1988) *Biochemistry 27*, 2450–2459.

Ohnishi, T., Schagger, H., Meinhardt, S. W., LoBrutto, R., Link, T., & von Jagow, G. (1989) *J. Biol. Chem. 262*, 735–744.

Paddock, M. L., Williams, J. C., Rougey, S. H., Abresch, E. C., Feher, G., & Okamura, M. (1986) *Prog. Photosynth. Res. 3*, 775–778.

Powers, L., Schagger, H., von Jagow, G., Smith, J., Chance, B., & Ohnishi, T. (1989) *Biochim. Biophys. Acta 975*, 293–298.

Prince, R. C., Bashford, C. L., Takamiya, K.-I., van den Berg, W. H., & Dutton, P. L. (1978) *J. Biol. Chem. 253*, 4137–4142.

Rao, J. K. M., & Argos, P. (1986) *Biochim. Biophys. Acta 869*, 197–214.

Rich, P. R. (1984) *Biochim. Biophys. Acta 768*, 53–79.

Rich, P. R. (1989) in *Highlights of Modern Biochemistry* (Kotyk, A., et al., Eds.) Vol. I, pp 903–912, V.S.P. Publishers, Prague.

Robertson, D. E., & Dutton, P. L. (1987) in *Cytochrome Systems: Molecular Biology and Bioenergetics* (Papa, S., Chance, B., Ernster, L., & Jaz, J., Eds.) pp 593–600, Plenum Press, New York.

Robertson, D. E., & Dutton, P. L. (1988) *Biochim. Biophys. Acta 935*, 273–291.

Robertson, D. E., Giangiacomo, K. M., deVries, S., Moser, C. C., & Dutton, P. L. (1984) *FEBS Lett. 178*, 343–350.

Robertson, D. E., Moser, C. C., Giangiacomo, K. M., deVries, S., & Dutton, P. L. (1985) *Biophys. J. 47*, 240a.

Robertson, D. E., Davidson, E., Prince, R. C., van den Berg, W. H., Marrs, B. L., & Dutton, P. L. (1986) *J. Biol. Chem. 261*, 584–591.

Romish, et al. (1987) in *Cytochrome Systems: Molecular Biology and Bioenergetics* (Papa, S., Chance, B., Ernster, L., & Jaz, J., Eds.) pp 303–308, Plenum Press, New York.

Rutherford, W. A., & Evans, M. C. (1980) *FEBS Lett. 110*, 257–261.

Saraste, M. (1984) *FEBS Lett. 166*, 367–372.

Siedow, J. N., Power, S., de la Rosa, F. F., & Palmer, G. (1978) *J. Biol. Chem. 253*, 2392–2399.

Sinning, I., Michel, H., Matis, P., & Rutherford, A. W. (1989) *Biochemistry 28*, 5544–5553.

Snozzi, M., & Crofts, A. R. (1984) *Biochim. Biophys. Acta 766*, 451–463.

Takamiya, K.-I., & Dutton, P. L. (1979) *Biochim. Biophys. Acta 548*, 309–327.

von Jagow, G., & Ohnishi, T. (1985) *FEBS Lett. 185*, 311–315.

von Jagow, G., & Link, T. (1986) *Methods Enzymol. 126*, 253–271.

Weber, S., & Wolf, K. (1988) *FEBS Lett. 237*, 31–34.

Widger, W. R., Cramer, W. A., Hermann, R. G., & Trebst, A. (1984) *Proc. Natl. Acad. Sci. U.S.A. 81*, 674–678.

Williams, J. C., Steiner, L. A., & Feher, G. (1986) *Proteins 1*, 312–325.

Wraight, C. A., & Shopes, R. J. (1989) in *Techniques and New Developments in Photosynthesis Research* (Barber, J., & Malkin, R., Eds.) pp 183–191, Plenum Publishing Corp., New York.

Youvan, D. C., Bylina, E. J., Alberti, M., Begusch, H., & Hearst, J. E. (1984) *Cell 37*, 949–957.

Zanonni, D., Prince, R. C., Dutton, P. L., & Marrs, B. L. (1980) *FEBS Lett. 113*, 289–293.